ANTAL KERPELY DOCTORAL SCHOOL OF MATERIALS SCIENCE & TECHNOLOGY

Study of Zr4/Cr3 Based Conversion Coatings on Aluminium Alloys

A Ph.D. Theses booklet submitted in the defense process for degree of

Doctor of Philosophy in the subject of Material Science and Technology

by

Kalaivanan Thirupathi

Consultant:

Prof. Dr. Pál Bárczy

Professor Emeritus

Space Material and Technology

Institute of Ceramics and Polymer Engineering

Faculty of Material Science and Engineering

University of Miskolc

Hungary, 2018

ABSTRACT

The aluminium and its alloys are used mostly for several industrial applications. Aluminium exhibits desirable mechanical properties resulting from addition of elements like Si, Cu, Mg etc. Some of the aluminium alloys exhibits good corrosion resistance property under normal atmospheric conditions. Protecting the surface of metals with a coating will improve its life expectancy. The hexavalent chromium coating is used till date because of a better corrosion resistance property. However, its toxic nature leads to immediate replacement with an ecofriendly coating. The Zr4/Cr3 based conversion coating has shown promising results that could possibly replace hexavalent chromate coatings. SurTec 650 RTU from SurTec ltd. is one of most leading zirconium based trivalent chromate solutions among potential alternatives. Therefore, this dissertation is focused on understanding the coating structure, influence of alloying elements in substrate during conversion process, effect of ageing and growth kinetics of the coating. The coating over three aluminium alloys namely AA6082-T651, AA2024-T351 and AA7075-T651 was selected for investigations because of the variation in alloying elements. The investigation was conducted by depth profiling of coated samples using secondary neutral mass spectroscopy and glow discharge optical emission spectroscopy. As a result, the structure of the coating was revealed by using high vacuum exposure. The influence of alloying elements in the substrate during conversion process was identified. The elemental level changes that occur in coating during ageing process was discussed. At last, the complete growth cycle of this conversion coating over an aluminium alloy was explained.

1 INTRODUCTION

Aluminium alloys like AA6082, AA2024 and AA7075 are widely used in aircraft and space construction metallic components due to their lightweight and mechanical properties [1]. It is necessary to protect metal surfaces with a coating that provides good resistance against corrosion and adhesion to top coats. Hexavalent chromium-based conversion coating is widely used for aluminium alloys. However its toxic, hazardous and carcinogenic nature of hex chrome compounds has led to an urgent need to find eco-friendly replacements, as mandated by various directives of the European Union [2]. Among potential alternative treatments, Zr4/Cr3 based conversion coating has shown promise [3]. This conversion coating is nowadays widely used for the protection of aluminium alloys [4]. The developments published, related to this conversion coating shown successful results in corrosion protection behaviour over aluminium alloys and provided good adhesion for paints.

This conversion bath usually consists of zirconium fluorides and trivalent chromium salts. The formation mechanism of this coating over AA2024 alloy has been studied for several years, it is now known that this process involves dissolution and redepositing of ions from the substrate as well as from the chromium bath with interfacial pH variation during the coating process [5][6]. Investigation on the growth of coating over AA2024 indicate that this coating consists of two layers, an outer layer containing a greater number of Zr and Cr species and inner layer rich of oxides and fluorides of aluminium [7][8].

In one study the impacts of ageing using AA2024 alloy as a substrate were studied and it was suggested that coating become more hydrophobic at elevated temperature [9]. While there are studies on the formation of coating over AA7075, research on the effect of high vacuum and ageing related to Zr4/Cr3 based conversion coating over AA6082 and AA7075 alloys is limited.

The structure of coating has not been studied or reported so far. A TEM image of coating over AA2024 shows that the coating is porous in nature [10]. However, not much is known about the impact of vacuum or influence of sample preparation. Published investigations about coating thickness measurements mentioned that under vacuum, coating undergoes severe dehydration.

Besides, the study about coating growth kinetics over super pure aluminium using AFM and TEM indicated that coating growth has three states: an active period up to 30 s, linear state lasting for 600 s and changes to limited growth after 1200 s [11]. The study was done on pure aluminium; thus the influence of alloying elements is not well defined. To discover, we have coated AA6082 alloy sample under various immersion time to predict growth kinetics of conversion coating inside the bath.

An investigation about formation of coating over AA2024 reveals that the coating has several cracks and detachment over the substrate. The coating over copper rich particles shows some change in formation as mentioned in literature [12]. This indicates that alloying elements have major contribution to the formation of the coating [13]. However, not many studies have been carried out previously to understand the influence of substrate composition in the formation of Zr4/Cr3 conversion coating. The effect of alloying elements in aluminium substrate was not investigated in the published papers related to this conversion coating.

1.1. Objectives

After detailed study of the most recent literatures, we have concluded to focus only on certain knowledge gaps. Our main interests were to identify the structure of the coating which was never described perfectly. Because of its vivid environmental sensitivity (time, temperature, pressure, humidity etc) and thin layering, the structure transforms continuously under laboratory environment from day to day. Furthermore, the vacuum environment inside the structure investigating devices like TEM (Transmission Electron Microscopy) and SEM (Scanning Electron Microscope) also generates further structural changes. The most sensitive depth profiling techniques such as SNMS (Secondary Neutral Mass Spectroscopy) and GD-

OES (Glow- Discharge Optical Emission Spectroscopy) was applied in this research work. There are four main aims to achieve, relating to the four activities listed below.

1. To study the role and contribution of alloying elements in the aluminium substrate during conversion process.
2. To understand the elemental structure changes that occur during ageing process, on the basis of investigations with SNMS apparatus.
3. To study the effect of high vacuum on the structure of this Zr4/Cr3 based conversion coating over aluminium alloy.
4. To study the growth kinetics of Zr4/Cr3 conversion coating over AA6082

2 EXPERIMENTAL SECTIONS

2.1 Sample preparation

Table 1. Elemental composition of investigated alloys

Wt. %	Zn	V	Ti	Sn	Si	Pb	Ni	Mn	Mg	Ga	Fe	Cu	Cr	Bi	Al
6082	0.01	0.01	0.01	0.007	1.09	0.003	0.005	0.17	0.99	0.008	0.237	0.092	0.008	0.002	96.7
7075	5.87	0.009	0.03	0.002	0.07	0.001	0.004	0.011	2.55	0.014	0.009	1.85	0.19	0.005	89.3
2024	0.06	0.004	0.05	0.006	0.09	0.003	0.005	0.55	1.63	0.01	0.18	4.86	0.01	0.004	92.7

The elemental composition of metal samples was determined by ICP-OES as mentioned in Table 1. The samples were obtained as 10x10 mm sheets with 4 mm thickness. The received specimens were initially cleaned with detergent and rinsed with isopropyl alcohol, ethanol, and acetone for few seconds. Mechanical polishing modified the surface of samples up to 800 grid finishes and then was electro polished using Struers electrolyte A2-I and II (50 v/v%) at 20 V for 60 s around 25˚C followed by rinsing using DI water, ethanol and drying in cool air stream. The degreased samples were etched with 5 v/v% of NaOH for 180 s and desmutted with H_2SO_4 solution of 17 v/v% for 180 s. Both pre-treatments were carried out at room temperature. The samples were thoroughly rinsed using deionised water after each pre-treatment.

Zr4/Cr3 conversion parameters

1. Sample Preparation: Elemental analysis of Zr4/Cr3 based conversion coating	
Alloy used	Etched and desmutted AA6082
Solution	SurTec 650
pH	3.8

Temperature	40˚C
Immersion time	600 s
Rinsing	Deionised water at room temperature
Drying	24 h before measurement
Instrument used	SNMS

2. Sample Preparation: Coating structure by exposure to vacuum	
Alloy used	Etched and desmutted AA6082
Solution	SurTec 650
pH	3.8
Temperature	40˚C
Immersion time	180 s
Rinsing	Deionised water at room temperature
Drying	24 h before measurement
Vacuum exposure	2 h at 10^{-7} mbar
Instrument used	GD-OES and SNMS

3. Sample Preparation: Effect of alloying elements in the substrate during conversion process	
Alloy used	Etched and desmutted AA6082 and AA2024
Solution	SurTec 650
pH	3.8
Temperature	40˚C
Immersion time	300 s
Rinsing	Deionised water at room temperature
Drying	24 h before measurement
Instrument used	GD-OES

4. Sample Preparation: Ageing effect	
Alloy used	Etched and desmutted AA6082 and AA7075
Solution	SurTec 650
pH	3.8
Temperature	40˚C
Immersion time	180 s

Rinsing	Deionised water at room temperature
Drying	24 h before measurement labelled as ‘‘Fresh’’
	168 h before measurement labelled as ‘‘Aged’’
Instrument used	SNMS

5. Sample Preparation: Growth Kinetics of the coating	
Alloy used	Etched and desmutted AA6082
Solution	SurTec 650
pH	3.8
Temperature	40˚C
Immersion timings	60, 300, 600, 720, 1440, 1920, 2280 s
Rinsing	Deionised water at room temperature
Drying	24 h before measurement
Instrument used	GD-OES

3 RESULTS AND DISCUSSION

3.1 Elemental analysis of coated sample using SNMS

Almost all the ions that is suspected to be present in the coating region was investigated by the SNMS. Figure 1 represents intensity vs atomic mass of elements detected from the coating. The graph indicates both ions from coating and substrate. The intensity on the y axis represents an approximate quantity of the ions in arbitrary unit. The carbon (12.0), oxygen (15.9), sodium (22.9), aluminium (26.9), silicon (28.0), sulphur (32), chromium (51.9), manganese (54.9), copper (63.5), zirconium (91) ions that were identified from the coated AA6082. This graph also indicates the concentration of Zr could be higher compared to Cr in the coating. Neglecting the ions from the substrate, we have concluded that zirconium, chromium, oxygen and aluminium are the major ions that exists in coating. The presence of carbon is possibly due to contamination from the vacuum chamber or mass spectrometer of SNMS device.

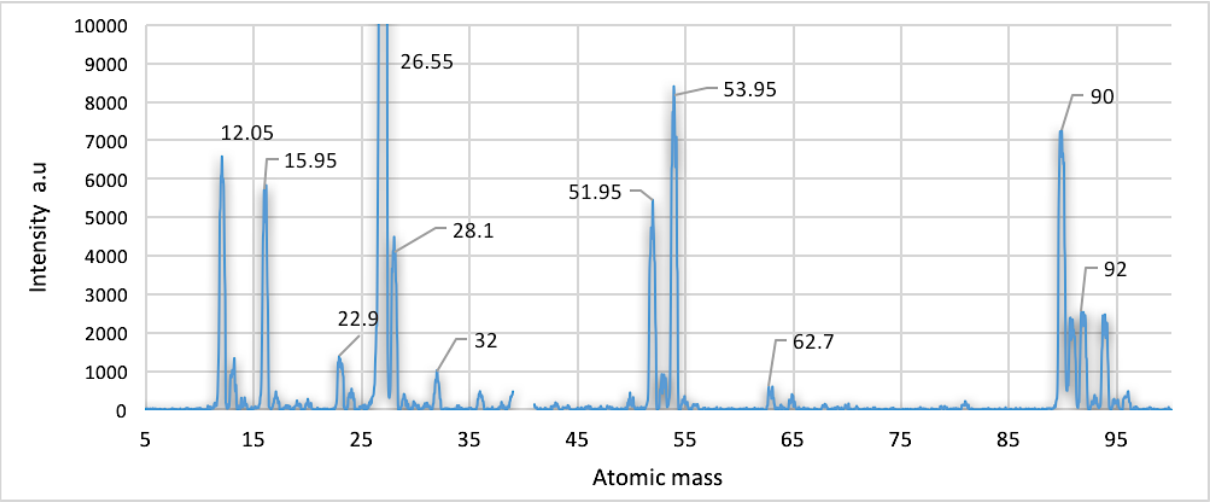

Figure 1. Elemental analysis of coated AA6082 using SNMS

However, some published journal papers states that fluoride ions does influence the formation mechanism of this coating over aluminium alloy [10]. In this analysis, we couldn't identify the presence of fluorides both in substrate and coating region. The presence of oxygen indicates that most ions in coating exist in form of oxides. The Figure 1 also indicates that the ions such as potassium and calcium cannot be identified by the SNMS due to usage of argon gas for sputtering of ions from the coating inside the vacuum chamber.

3.2 SNMS depth profile analysis

A typical layer structure of a coated AA6082 alloy is shown in Figure 2. The intensity was measured in arbitrary unit indicating the relative number of detected atoms. As seen in Figure 2, the oxygen content tends to decrease, but it is retained inside the layer. The aluminium curve indicates a different behaviour. On the surface, its value is minimum, but after leaving the layer, a sharp increase is observed up to a maximum, with no further change beyond a depth of 200 nm. The zirconium and chromium curves shows elongated peaks at 30–80 nm depths, with a slow transient toward increasing depths. We interpret these curves up to their peaks to represent the coating area, while the deeper part of the curve is believed to be a phantom segment caused due to surface roughness. The SNMS figures also confirm the absence of a sharp transition between the substrate and coating. We interpret that the ~0.34 µm surface roughness of the coated samples decreases the depth resolution, thus elongating interfacial regions in the curves.

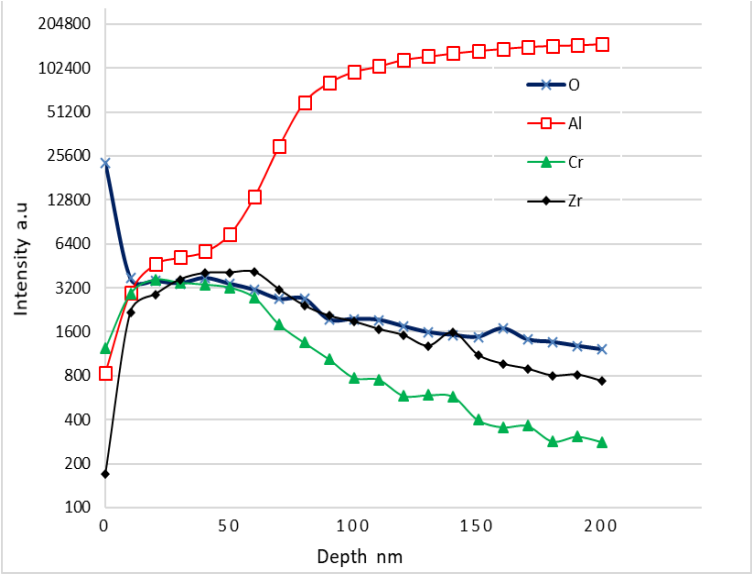

Figure 2. Typical SNMS atomic distribution in coated AA6082 alloy

3.3 GD-OES depth profile analysis

The Figure 3 shows elemental analysis of coating over AA6082 alloy for 600 s immersion time. The first peak in graph indicates the point where the sputtering of coating begins, and second peak represents interface between the coating and the substrate. In this report thickness of the coating was considered as the distance between the two peaks. It is obvious, that our interpretation is approximate since after the second peak around 300 nm there is a decreasing tendency for Zr, Cr and O curves with slight increase in alloying elements such as Mg, Cu curves. So, we can conclude that the coating thickness of this sample is around 300 nm. It is also observable from the Figure 3 that there is no sharp transition zone possible due to limitation in accuracy of measurement device.

The legend indicates the list of elements used for coating analysis using GD-OES. The ions that does not show any significant variation before second peak is considered as not available in the coating region. The intensity values on Y axis are an arbitrary unit which does not represent the exact elemental composition of coating. Instead of that, shapes of curve are analyzed to detect changes in coating composition. Both the Zr and Cr curve exhibited similar shapes. Because of the slight Cr content in substrates, only Zr distribution curves is considered for the analysis of coating and thickness measurements.

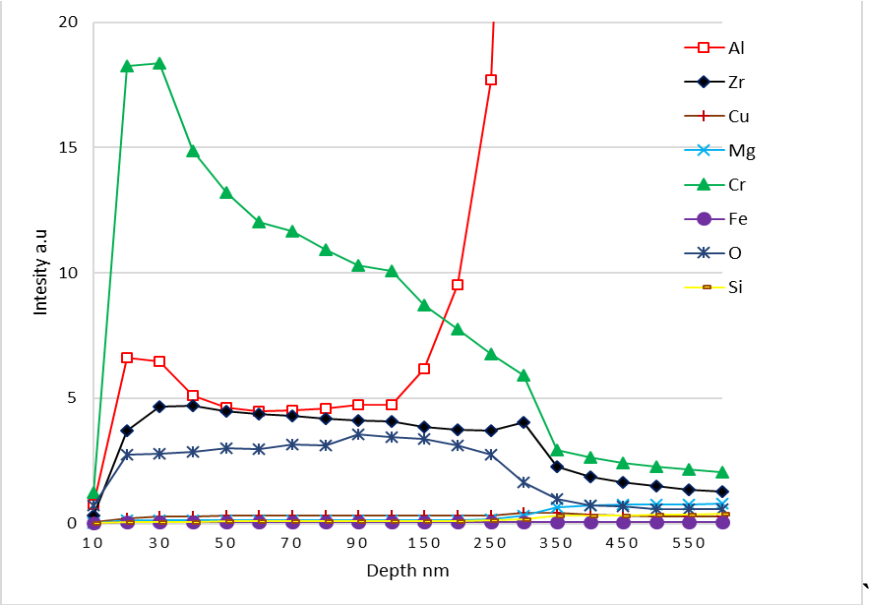

Figure 3. Typical GD-OES atomic distribution in coated AA6082 alloy

3.4 Structure of coating

Figure 4 represents the concentration distributions of Al, Cr, Zr and O ions as a function of sputtering time at fresh state over an AA6082 sample. The Cr and Zr curves have peaks, whereas the O and Al curves show monotonous decreasing or increasing trends. The concentration distribution for another AA6082 sample analysed after high vacuum treatment is shown in Figure 5. Comparing these figures, the O curve does not significantly change, but the Al and Cr curves radically decrease after high vacuum exposure. Interestingly, Zr ions completely disappear from the layer. In addition, layer shrinkage is also apparent after comparing both figures.

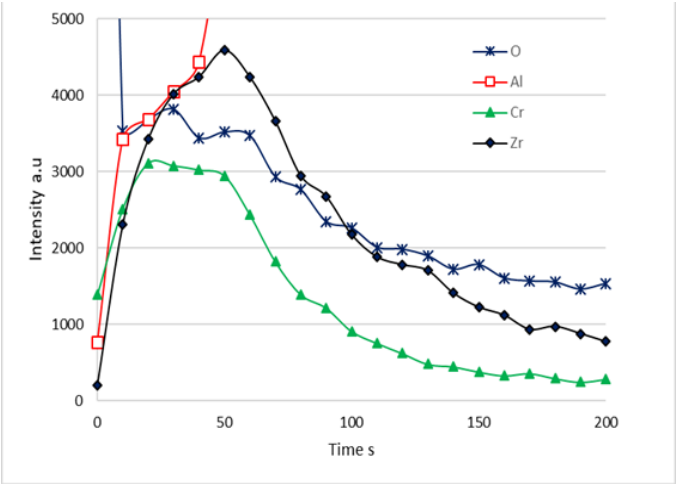

Figure 4. Atomic distribution in a coated AA6082 from SNMS prior to vacuum exposure (sol-gel structure)

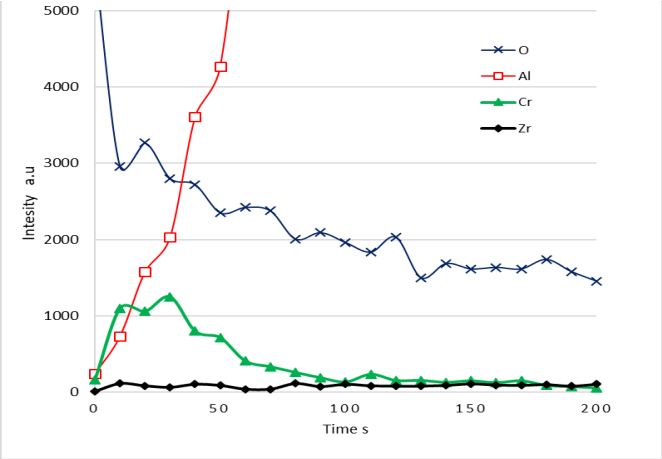

Figure 5. Atomic distribution in a coated AA6082 from SNMS after high vacuum treatment (gel structure)

To interpret these phenomena, we assume that the coating has a two-phase structure. The first phase is the -Al-O-Cr- molecular chain, building a gel-like network. The second is a low-viscosity sol phase, composed of mostly Zr with a few Cr ions from the coating bath and some Al ions from the substrate. This second phase proved to be removable from the network under high vacuum. The layering process seems to follow interesting kinetics. Electron interchange toward Cr ions begins with Al ions near the surface of the substrate, leading to molecular chain growth. Some Al ions from the solute can travel through the filtering network and dissipate in the sol phase. The nature of this sol phase is not fully understood. We assume that the Zr ions are surrounded by hydroxides in a cluster-like behaviour, in which some of the Cr and Al ions are in sol state. In summary, the conversion coating has a two-phase sol-gel structure that is observed after exposure to vacuum. A similar sol-gel effect has been observed from the depth profiling using GD-OES of coated samples that were exposed to high vacuum as explained below.

The Figure 6 shows the distribution of ions in coating that is formed over AA6082 alloy coated for 180 s. The graph represents that O, Cr, and Zr curves has high intensity up to 3 s after which there is a decrement, whereas the aluminium curves has less intensity for first few seconds after which it plummets in to higher. It is also significant from this graph that other alloying elements were not present in the coating region. Interestingly, the same coating over another sample is exposed to high vacuum reveals that there is a slight decrement in Cr, O and Al curves with complete disappearance of the Zr in coating as shown in Figure 7. Comparing Figure 6 and Figure 7 the disappearance of second peak is probably due to the tremendous shrinkage in coating after vacuum exposure [14].

We interpret these phenomenal changes by assuming that coating has two different phases as mentioned earlier from SNMS curves. The first is the -Al-Cr-O- phase that is in gel form. The second phase is in low viscosity sol form that mostly consists of Zr ions with smaller amount of Cr and Al ions. This second phase can be removed from the coating by exposure to high vacuum. Based on these results from GD-OES and SNMS curves we predict a simplified atomic model of Zr4/Cr3 based conversion process in the coating bath.

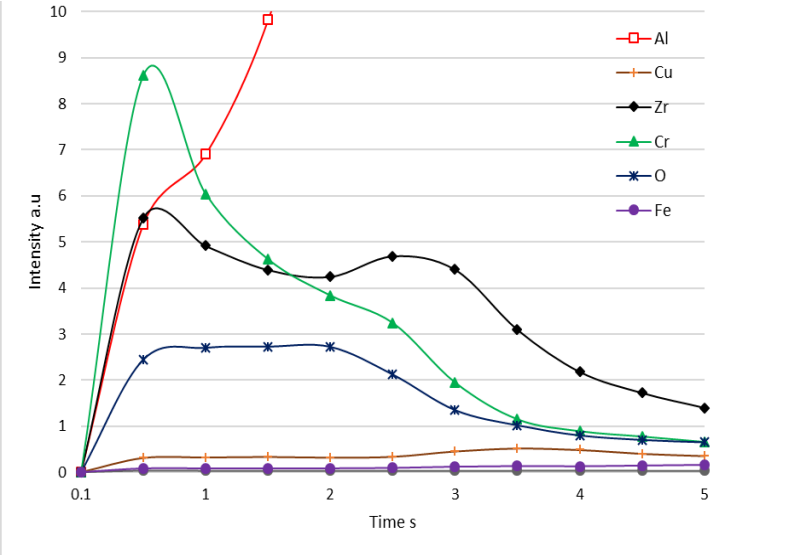

Figure 6. Atomic distribution in a coated AA6082 from GD-OES prior to vacuum exposure (sol-gel structure)

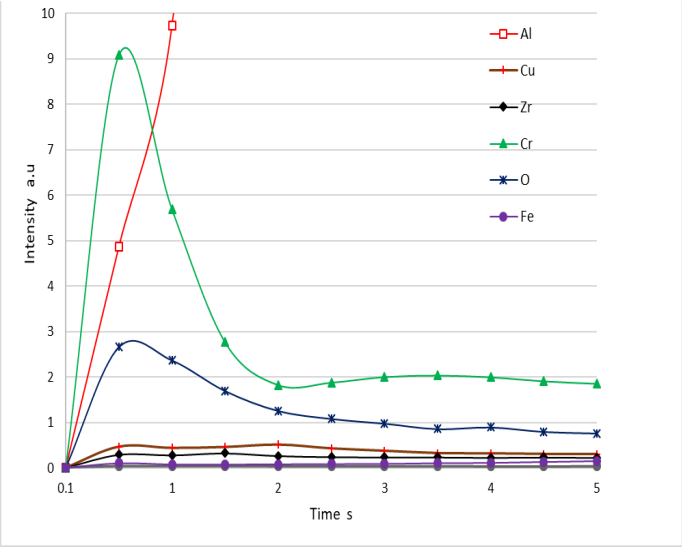

Figure 7. Atomic distribution in a coated AA6082 from GD-OES after high vacuum treatment (gel structure)

3.5 Simplified atomic model

After pre-treatment, the samples were immersed in to the coating bath. Almost all ions from the substrate and coating bath is somehow involved in the coating formation process. However, $Cr^{3+,}$ Zr^{4+} ions in the coating bath and Al^{3+} ions from the substrate does a major contribution in the ion exchange process. The slight change in temperature and an appropriate variation in interfacial pH due to the dissolution of the aluminium from the metal to Al^{3+} ions as shown in Figure 8 initiates the formation mechanism of coating. This is because Al^{3+} ions are stable in aqueous solution from aluminium Pourbaix diagram [15]. The Zr^{4+} and Cr^{3+} ions already exist inside the coating bath reacts with aluminium ions converts the surface of aluminium alloys into a complex mixture of all the three ions in various forms such as oxides, hydroxides, sulphates, and fluorides [7]. The layering kinetics starts near the surface of aluminium by formation of molecular chain of complex mixture Al, Cr and O components. The Zr^{4+} ions are mostly kept its solute state throughout the conversion process and it is assumed to be surrounded by hydroxides having a cluster like behaviour. Interestingly, some parts of Al filtering through the molecular oxide chain film and dissipated into sol phase. Finally, the detailed information about various chemical reactions that involve in complete formation mechanism coating over AA2024 could be obtained from literature [7]. In summary, it is stated that the formation mechanism of Zr4/Cr3 based conversion coating is highly depending on the standard electrode potential of that alloying elements in the substrate. The dissolution of aluminium in to the coating bath determines the formation mechanism of coating and its growth. This dissolution process is decelerated or promoted by the alloying elements in the substrate resulting in layer formation. Figure 8, also represents that the dissolution of aluminium ions is more for AA6082 compared to AA2024

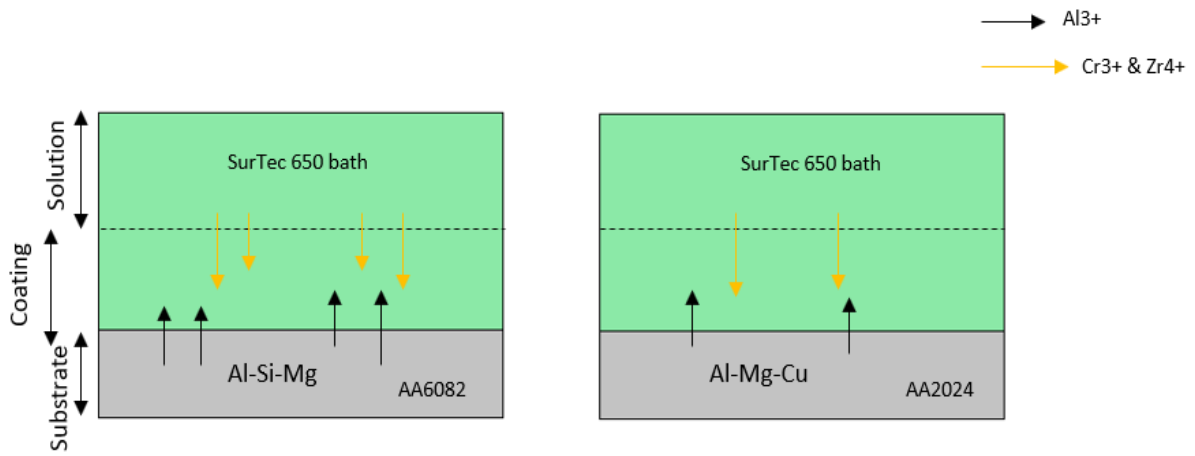

Figure 8. Simplified sketch of conversion process inside coating bath

3.6 Effect of alloying elements in the substrate during conversion process.

To study the effect of alloying elements during the conversion coating a series of coated samples were examined by GD-OES under same experimental parameter. The Figure 10 shows the distribution of aluminium and zirconium in coatings over AA6082 and AA2024 alloys after immersion in to the SurTec 650 bath for 300 s. The graph indicates that under same immersion time, aluminium dissolution is less, and the layer is thinner with less zirconium for AA2024 compared to AA6082. Since AA2024 is highly alloyed by copper ions, we predict that it disturbs the dissolution rate of Al ions. Whereas in case of AA6082 the dissolution rate is high which is the root cause for thicker coating growth under various immersion times. Over all, the dissolution process is depends up on the standard reduction potential of ions that is evident from literature [16]. The Si (-1.7 V) and Al (-1.6 V) has higher values in comparison to Cu (+0.15 V). The Si ions gives priority for dissolution of aluminium more inside the solution compared to Cu ions. This causes the variation in coating thickness formation over two alloys as shown in Table 2 . The Figure 9 represents the variation in coating thickness under various immersion time for three different aluminium alloys. This graph also indicates that highly alloyed substrate has low coating thickness under various immersion times compared to low alloyed substrate.

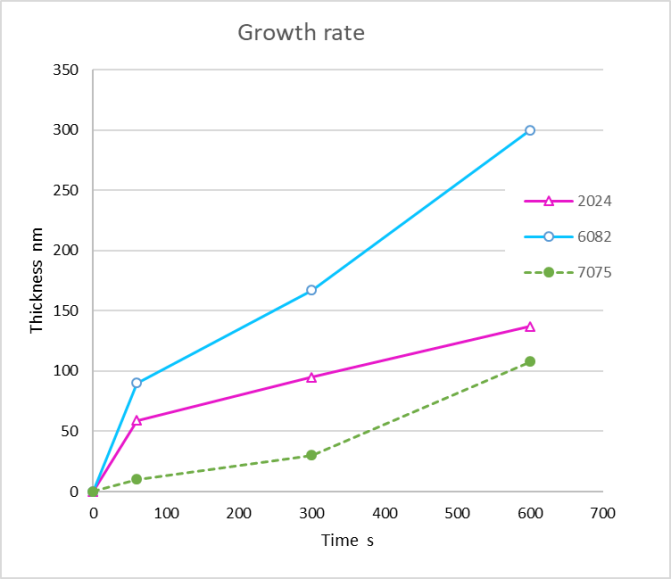

Figure 9 : Variation in thickness of coating under various immersion time.

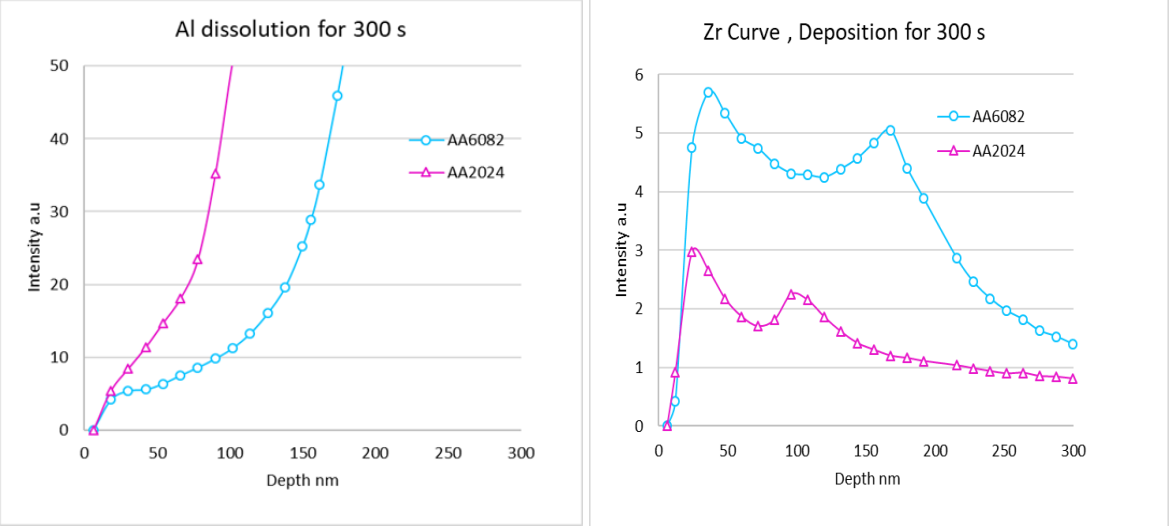

Figure 10. Aluminium dissolution and Zr deposition in coating over AA6082 and AA2024 alloys after 300s immersion time

Table 2. Coating thickness variation (nm) for two different alloys

	0 s	**60 s**	**300 s**	**600 s**
AA2024	0	59	95	137
AA6082	0	90	167	300

Table 2 indicates the variation in thickness of coating of AA6082 and AA2024 alloy with increase in immersion time. It is evident, from this table that the thickness of coating increases with immersion time. From these results, our hypothesis is that the layer formation seems to be highly dependent on the quantity of alloying elements in the substrate over coating is formed. The high alloyed substrate seems to have low coating thickness compared to low alloyed substrate. The aluminium dissolution determines the coating thickness.

3.7 Ageing

The effects of ageing have not been studied in detail previously , but there are certain literature claiming that ageing plays a major role in conversion coating behaviour [5]. The ageing process means drying the coating for a certain period of time to achieve the proper structure. We studied the ageing effect using SNMS to discover the structural transformation. The fresh and aged SNMS curves showed that the oxygen curve is drastically reduced inside the coating for the AA7075 alloy during the ageing process, as seen in Figure 11 (a, b). This finding signifies that there are some changes at an elemental level during the ageing process. In addition, other curves like Zr and Cr do not undergo any major changes. In the fresh state, the coating formed over

AA7075 has a higher oxygen curve compared to that of AA6082. We assume that the sol-gel proportion is a probable reason for this variation. It is also observed from Figure 11 (c and d) that the aluminium content of the AA6082 alloy is slightly reduced after ageing. From this SNMS analysis of fresh and aged samples, we predict that there is a change in the chemical state of the coating. A previous report suggests that the coating undergoes dehydration in the ageing process [9]. Our hypothesis is that once the samples are taken out of the bath, the coating undergoes a continuous transition from sol to gelatinous state. Based on the results of the high vacuum exposure, we found that mostly Zr ions are in sol form, with some Al and Cr ions. In summary, atoms in the coating tend to change their nature from sol to gelatinous states during the ageing process. This sol-gel transformation at room temperature appears to take a surprisingly long time (weeks or months), most probably caused by the slow Zr clusters.

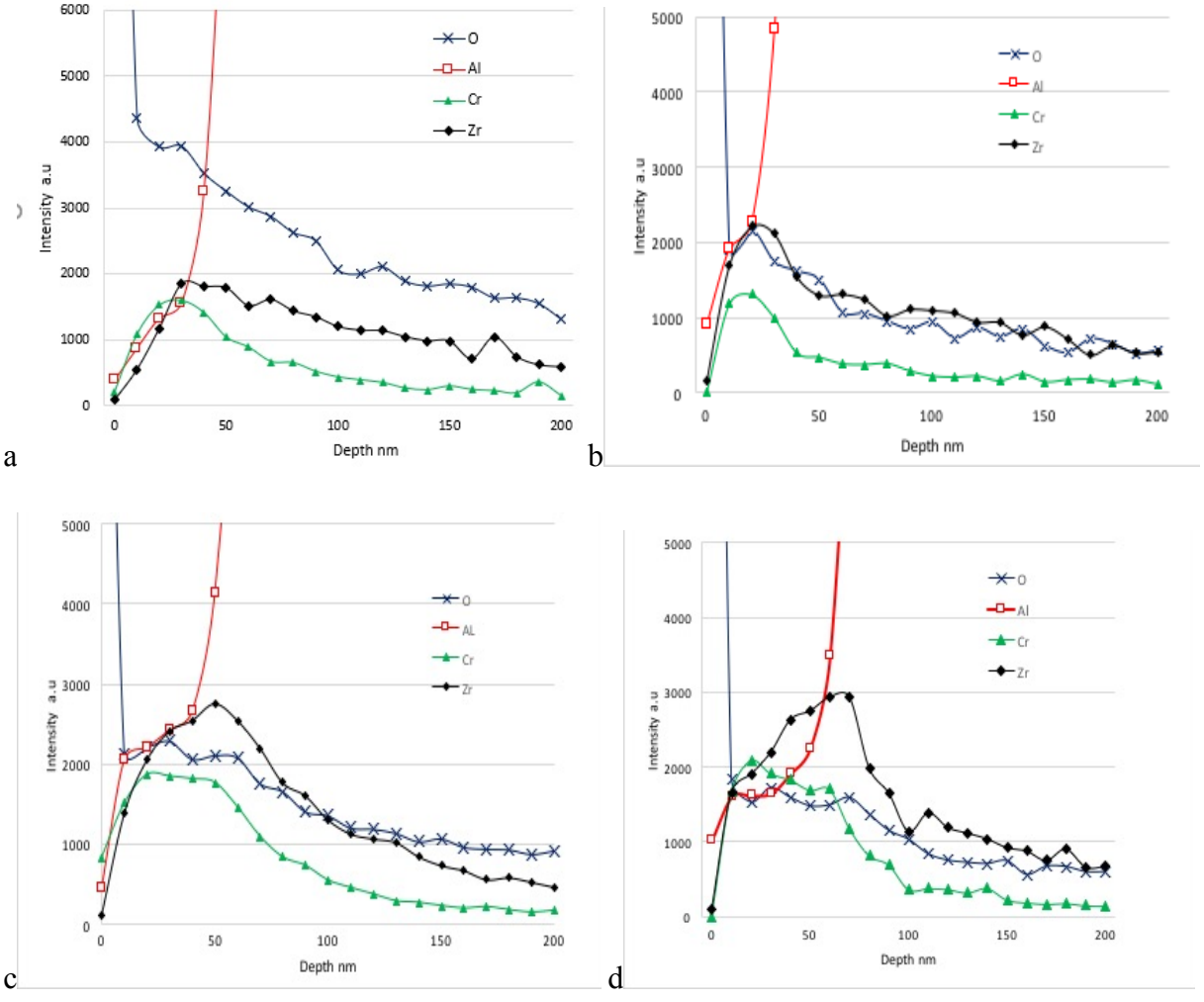

Figure 11. Atomic distribution in fresh (graph a, c) and aged (graph b, d) of coating formed over AA7075 and AA6082

3.8 Coating growth cycle

The growth cycle of conversion coating was investigated by measuring the thickness of coating with the function of immersion time. Comparing other two alloys AA6082 had high coating thickness which tends to study growth kinetics of Zr4/Cr3 based conversion coating using this alloy. Figure 12 shows five Zr distribution curves elucidating that the coating reaches maximum thickness of 450 nm around 1440 s after that there is a tremendous change in the shape of the curve. The coating growth process obviously ceased. The experimental results summarized in Table 3 represents the variation of coating thickness in function of immersion times.

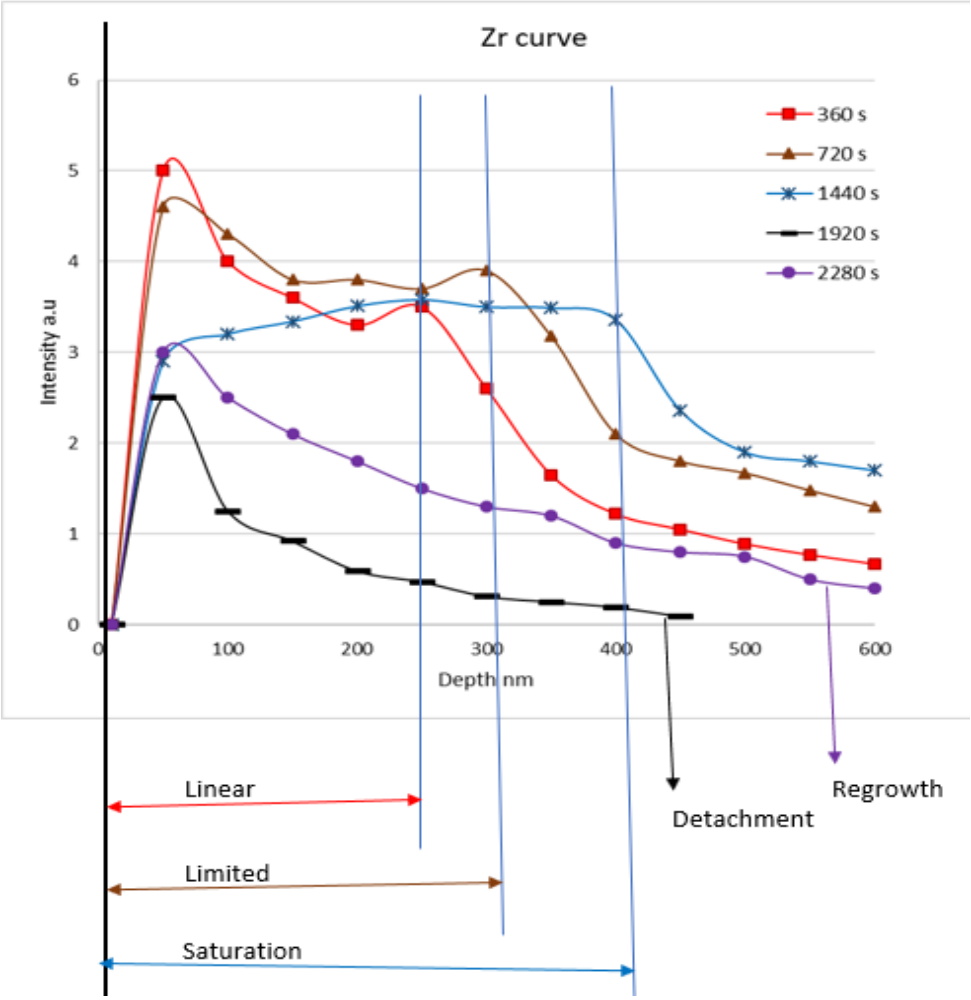

Figure 12. Zr distribution in example coatings formed over AA6082 that removed from coating bath after different immersion time

Table 3.Thickness of coating formed over AA6082 alloy under various immersion time

State	Time s	Coating thickness (nm)
Activation	0-60	0 – 100

Linear	60-540	~100 -310
Limited	540-900	~310-400
Saturation	900-1440	~450
Detachment	Above 1440	~55

Based on these data, we propose a coating growth model consisting of five different states. The Figure 13 represents the growth cycle of Zr4/Cr3 based conversion coating over AA6082 alloy.

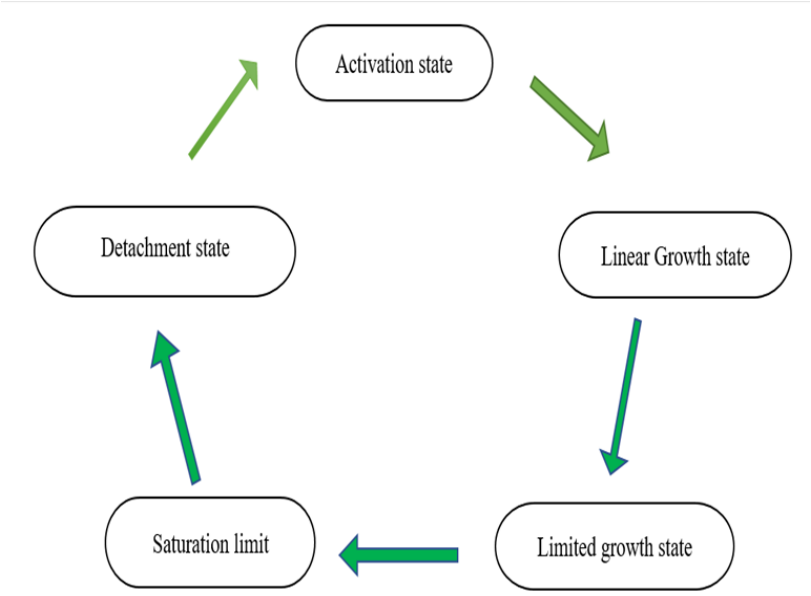

Figure 13. Coating growth cycle

The coating growth consist of five different state that is activation state, linear growth state, limited growth state, saturation and detachment state.

- The activation state is the initial period, when the aluminium starts its dissolution and thus the conversion process begins. The coating reaches a maximum of 100 nm during this state. The state starts quickly below 60 s.
- Linear growth state is the period where the formation of coating is higher. The aluminium dissolution inside the coating bath is abundant and a rapid conversion process occurs over the surface of alloy. Almost, entire surface of the substrate is covered with a long molecular chain network of Cr, Zr, Al and O ions.
- Limited growth rate is the state where the aluminium dissolution is disturbed by the coating that is previously formed over the substrate. This reduces further formation of the coating because there not much Al ions that can pass through molecular network to

react with Cr3 and Zr4 ions in the coating bath. We assume that the aluminium somehow dissolute in certain regions like cracks that tends to contribute coating growth. The growth of coating is very slow during this state compared to the previous two states.

- Saturation limit is the point where there are no more ions dissolutes from the substrate. The coating reaches its maximum limit, beyond that there is no more coating growth. This saturation limit is varying according to the size of the sample and its composition. Over all, most of the samples reached this limit approximately at 450 nm. The saturation limit can occur at different time and coating thickness over samples. We conclude that for AA6082 sample with thickness mentioned earlier has saturation limit reaches around 1440 s after which the next state begins
- Detachment state is point the where the coating is dispatched from the substrate and disappears in the coating bath. We predict that after saturation limit the coating cracks in several place and large agglomerates of Cr, Zr and Al ions in coating dispatches from the surface of alloy. However, the chemistry behind this dispatch is unknown. The coating thickness measured beyond this detachment state represents the regrowth of coating.

4 CONCLUSION

4.1 LIST OF THESES WORK

4.1.1 COATING STRUCTURE

Based on the SNMS and GD-OES measurements, we found that the Zr4/Cr3 based conversion coating exhibits sol-gel type structure. The conversion coating over AA6082 aluminium alloy is in sol and gelatinous states that were found separable under exposure to the high vacuum. The sol part mostly consists of Zr and small amount of Cr, Al, and O solute in water. Whereas the gel phase constitutes a large molecular network of Cr-Al-O. However the double layer coating structure on AA2024 [10][7] was not confirmed on AA6082 and AA7075.

4.1.2 IMPORTANCE OF Al DISSOLUTION IN CONVERSION PROCESS

The formation mechanism of Zr4/Cr3 based conversion coating is highly dependent on the standard potential of the alloying elements in the substrate. The dissolution of aluminium in to coating bath determines the formation of coating and its growth. This dissolution process is decelerated and halted by the alloying elements like copper in the substrate resulting in a thin layer with a low chromium content.

4.1.3 SUBSTRATE INFLUENCES IN CONVERSION PROCESS

In comparison with other two alloys, AA6082 alloy tends to have high coating thickness. The depth profiling of coating over AA6082 and AA2024 alloys showed that the substrate which is highly alloyed has low coating thickness with less zirconium content. In case of AA2024, the dissolution of aluminium ions in bath is decelerated by neighbouring copper ion resulting in low thickness coating formation with less chromium and zirconium.

4.1.4 AGEING EFFECT

The fresh conversion coating is not stable and there are structural changes in the composition of coating under normal atmospheric condition. The depth profiling of coating formed over AA6082 and AA7075 under both aged and fresh state using SNMS reveals the changes that occur inside the coating. The reduction in oxygen and variation in aluminium intensity under ageing process indicates that the coating undergoes a continuous transformation from sol to gel.

4.1.5 COATING GROWTH

Under sample preparation technique 5, the study about the growth kinetics of Zr4/Cr3 based conversion coating over AA6082 alloy reveals the cycle of the coating growth. The growth kinetics consist of the activation, linear, limited, saturation and detachment states. The results obtained from depth profiling of coated AA6082 samples at various immersion indicates that after the detached state there is a possibility for regrowth of coating. Once coating is detached from the substrate the aluminium ions over surface dissolutes again and regrowth occurs.

5 Publications related to this thesis work

5.1 Scientific publication

1. K. Thirupathi, P. Bárczy, and B. M. Somosvári, “Impact of Corrosive Liquid on Trivalent Chromium over Aluminium Alloys,” Journal of Surface Engineered Materials and Advanced Technology, vol. 7, no. 3, pp. 51–60, 2017.
2. K. Thirupathi, P. Bárczy, and G. Lassu, “Growth Kinetics and Structure of Zr4 / Cr3 Based Conversion Coating over Aluminium,” Functional Nanostructure, vol. 1, no. 3, pp. 114–119, 2017.
3. K. Thirupathi, P. Bárczy, and B. M. Somosvári, “Eliminating Hexavalent Chromium in Conversion Coating for Space Application,” in 5th Interdisciplinary doctoral conference, 2016, pp. 201–215.

4. K. Thirupathi, P. Bárczy, K. Vad, A. Csik, and B. Márton Somosvári, "Effects of Vacuum and Ageing on Zr4/Cr3 based Conversion Coatings on Aluminium Alloys," Applied Surface Science, vol. 441, pp. 1043–1047, 2018.
5. K. Thirupathi, P. Bárczy, B. M. Somosvári, and T. Bárczy, "Hexavalent chromium free coatings for satellite metallic hardware's," in 3rd International conference on research, technology, and education of space, 2017, pp. F-35.

5.2 Oral and Poster Presentations

1. 2016, 5th Interdisciplinary Doctoral Conference May 27 -29, Pecs, Hungary, Oral Presentation on Eliminating Hexavalent Chromium in Conversion Coatings for Space Application.
2. 2017, 3rd International Conference on Research, Technology and Education of Space, February 9-10, Budapest, Hungary, Oral Presentation on Hexavalent Chromium Free Coatings for Satellite Metallic Hardware
3. 2017, 2nd International Conference on Applied Science, June 12-15, Dalian, China, Poster Presentation on Study of Trivalent Chromate Coating on Aluminium Alloys by SNMS.
4. 2017, 3rd International Conference on Surfaces, Coatings and Nanostructured Materials, December 4 -7, Hong Kong, China, Oral Presentation on Effects of Vacuum and Ageing on Zr4/Cr3 based Conversion Coatings on Aluminium Alloys.

6 REFERENCES

[1] I. J. Polmear, *Light Alloys*. Edward Arnold, 2005.

[2] European Union, "Proposal for a Directive of the European Parliament and of the Council on the Restriction of the Use of Certain Hazardous Substances in Electrical and Electronic Equipment - Impact Assessment," 2008. .

[3] S. A. Kulinich and A. S. Akhtar, "On conversion coating treatments to replace chromating for Al alloys: Recent developments and possible future directions," *Russ. J. Non-Ferrous Met.*, vol. 53, no. 2, pp. 176–203, 2012.

[4] E. J. Smith, H. A. Al-Sanawi, B. Gammon, P. J. St. John, D. R. Pichora, and R. E. Ellis, "Volume slicing of cone-beam computed tomography images for navigation of percutaneous scaphoid fixation," *Int. J. Comput. Assist. Radiol. Surg.*, vol. 7, no. 3, pp. 433–444, 2012.

[5] L. Li, "Corrosion Protection Provided By Trivalent Chromium Process," *Thesis*, 2013.

[6] L. Li and G. M. Swain, "Formation and structure of trivalent chromium process coatings on aluminum alloys 6061 and 7075," *Corrosion*, vol. 69, no. 12, pp. 1205–1216, 2013.

[7] J. T. Qi, T. Hashimoto, J. R. Walton, X. Zhou, P. Skeldon, and G. E. Thompson, "Trivalent chromium conversion coating formation on aluminium," *Surf. Coatings Technol.*, vol. 280, pp. 317–329, 2015.

[8] J. Qi, A. Němcová, J. R. Walton, X. Zhou, P. Skeldon, and G. E. Thompson, "Influence of pre- and post-treatments on formation of a trivalent chromium conversion coating on AA2024 alloy," *Thin Solid Films*, vol. 616, pp. 270–278, 2016.

[9] L. Li and G. M. Swain, "Effects of aging temperature and time on the corrosion protection provided by trivalent chromium process coatings on AA2024-T3," *ACS Appl. Mater. Interfaces*, vol. 5, no. 16, pp. 7923–7930, 2013.

[10] J. Qi, T. Hashimoto, J. Walton, X. Zhou, P. Skeldon, and G. E. Thompson, "Formation of a Trivalent Chromium Conversion Coating on AA2024-T351 Alloy," *J. Electrochem. Soc.*, vol. 163, no. 2, pp. C25–C35, 2016.

[11] J. Qi and G. E. Thompson, "Comparative studies of thin film growth on aluminium by AFM, TEM and GDOES characterization," *Appl. Surf. Sci.*, vol. 377, pp. 109–120, 2016.

[12] R. Grilli, M. A. Baker, J. E. Castle, B. Dunn, and J. F. Watts, "Corrosion behaviour of a 2219 aluminium alloy treated with a chromate conversion coating exposed to a 3.5% NaCl solution," *Corros. Sci.*, 2011.

[13] L. Li, D. Y. Kim, and G. M. Swain, "Transient Formation of Chromate in Trivalent Chromium Process (TCP) Coatings on AA2024 as Probed by Raman Spectroscopy," *J. Electrochem. Soc.*, vol. 159, no. 8, pp. C326–C333, 2012.

[14] K. Thirupathi, P. Bárczy, K. Vad, A. Csik, and B. Márton Somosvári, "Effects of Vacuum and Ageing on Zr4/Cr3 based Conversion Coatings on Aluminium Alloys," *Appl. Surf. Sci.*, vol. 441, pp. 1043–1047, 2018.

[15] Joseph Edwards, *Coating and surface treatment systems for metals:* ASM International, 1997.

[16] M. Clugston and R. Flemming, *Advanced Chemistry*. Oxford university press, 2000.